

2021 IEEE Intelligent Vehicles Symposium (IV 2021)

Accepted paper. Accepted June 2021

© 2021 IEEE. Personal use of this material is permitted. Permission from IEEE must be obtained for all other uses, in any current or future media, including reprinting/republishing this material for advertising or promotional purposes, creating new collective works, for resale or redistribution to servers or lists, or reuse of any copyrighted component of this work in other works.

# Comparative Study of Prediction Models for Model Predictive Path-Tracking Control in Wide Driving Speed Range

Mizuho Aoki<sup>1</sup>, Kohei Honda<sup>1</sup>, Hiroyuki Okuda<sup>1</sup> and Tatsuya Suzuki<sup>1</sup>

**Abstract**—This study compares and evaluates the effect of the choice of the vehicle’s prediction model on the performance in designing a path-tracking controller for vehicles using Model Predictive Control (MPC). The Kinematic Ackermann Model (KAM), the Kinematic Bicycle Model (KBM), and the Dynamic Bicycle Model (DBM) are well known as nonlinear prediction models. The stability and tracking performance of these models are evaluated using simulations, and a newly proposed DBM improved in Low-speed range (DBM-L) is also compared.

As a result of the simulation, the proposed DBM-L was able to run in the widest 0 to 120km/h speed range among the models tested, and it was able to achieve the stop-and-go behavior that was not possible with the conventional DBM.

In the future, if we can solve the problem that the tracking accuracy of the DBM-L is slightly decreased in the extremely low and high speed ranges, a vehicle prediction model that can be used in all speed ranges is expected to be realized.

## I. INTRODUCTION

Autonomous driving technologies have attracted great attention in this decade, and a huge number of innovations are made as the results of numerous researches and developments carried out by academia and industry. It is obvious that the environmental recognition and the localization technologies turn the guided automatic vehicle control to the autonomous driving due to the development of LiDAR sensor and the AI-based image processing technologies. On the other hand, the motion planning and control are still important as the fundamental component supporting the overall autonomous driving system. Control stability and smoothness are critical issues on the automatic vehicle control not only to realize reliable autonomous vehicles but also to improve the passengers’ riding comfort.

Another aspect required for the vehicle control for an autonomous driving system is accuracy. In the context of autonomous driving, vehicle control is mainly used to track the local reference generated by the motion planner depending on the driving task targeted in the driving situation (See Fig.1). Inaccurate vehicle control may make the planned path meaningless even if the perfect local reference is generated to realize safe or comfortable driving. Although this problem can be solved by tuning the path planner to be robust and conservative, this approach increases the development or computational cost of the path planner. In addition, the test or validation cost for path planner is especially increased since it is difficult to determine whether the problem is caused by the vehicle controller or the path planner itself.

Realization of accurate vehicle control is a basic but still fundamental concern to reduce the total development cost for autonomous driving systems. There is much literature for vehicle control for autonomous driving, such as pure pursuit [1], rear-wheel position feedback [2] and the look-ahead control [3] standing on the classic feedback control. Although these approaches are simple, practical, and well-known control approaches, they often require a fine adaptive parameter tuning to realize stable driving in various road conditions and speeds.

Recently, a real-time optimization-based control method called model predictive control (MPC) [4] [5] has been attracting attention. MPC determines the control input by solving an open-loop optimal control problem (OCP) for a finite time ahead using a prediction model of the control target in real-time. The big advantage of MPC is the ability to impose various constraints on control inputs and states. As long as the prediction model is given with sufficient accuracy, MPC computes the optimal input in terms of the evaluation function of the optimization problem with satisfying those constraints. Generally speaking, the accuracy of the prediction model is critical in the MPC controller design. Since the vehicle model is nonholonomic in nature and contains various non-linearity, one of MPC design approaches is applying a linear approximation [6] [7] to the vehicle model. While linearization leads to the reduction of the computational cost and make the stability analysis easy, the performance of path tracking is degraded at the same time.

In recent years, Nonlinear MPC (NMPC) has been used to track vehicle paths using nonlinear vehicle models. Typical models used in nonlinear MPC path-tracking are the Kinematic Ackermann Model (KAM), the Kinematic Bicycle Model (KBM), the Dynamic Bicycle Model (DBM) [8] [9], and so on. Each of these models expresses the lateral motion of the vehicle under several assumptions. Likewise, it is necessary to consider the longitudinal motion, and constant acceleration is often assumed to make the problem simple. Thus, this paper focuses only on the lateral control, i.e. steering control, of the vehicle but not the longitudinal control, i.e. acceleration/deceleration control.

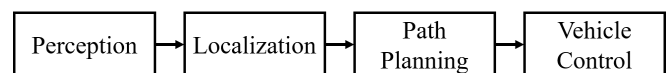


Fig. 1. Flow of autonomous driving

<sup>1</sup> M. Aoki, K. Honda, H. Okuda, and T. Suzuki are with Department of Mechanical System Engineering, Nagoya University, Furo-cho, Chikusa-ku, Nagoya, Aichi, Japan, e-mail: aoki.mizuho@i.mbox.nagoya-u.ac.jp

Although path tracking using the above vehicle models has been tried in much literature [10]–[14], quantitative comparison between different prediction models are not carried out for the specified driving task. The clear discussion and knowledge about which model should be chosen must accelerate the design of a practical path-tracking controller.

Polack et al. [15] investigated the model accuracy of the KBM comparing to real car behavior and found that the prediction error increased with vehicle speed and acceleration. Kong et al. implemented MPC with the KBM and MPC with the DBM on a real vehicle and compared the control performance, concluding that the KBM is more suitable for tracking control in their specified speed range. These studies are based on real vehicle experiments and the results are remarkable, however, the tested driving speed ranges are limited. Demand for the MPC controller is now extending from a simple highway cruising application to more various driving tasks including urban driving and the parking situation. It is necessary to share the knowledge about which prediction model should be appropriate for a particular driving speed range through a more comprehensive comparative study.

This paper presents a comparison of lateral vehicle models as prediction models in the context of MPC over a wide range of driving speeds. For the practical application of MPC to real-world vehicle control, the models are evaluated from the following perspectives, 1. sufficiently high calculation speed for practical use, 2. stable over a wide range of driving speeds for practical use in various driving situations, 3. stable over a wide tuning range of parameters to achieve the desired path-tracking characteristics. One contribution of this study is that these nonlinear models are compared in a common framework of NMPC using Continuation/Generalized Minimum Residual (C/GMRES) [16] method to implement and evaluate them in a practical computational time. In addition, we also propose a new DBM improved in Low-speed range (DBM-L) that is improved to prevent the DBM from diverging in the low-speed region, and evaluate its effectiveness.

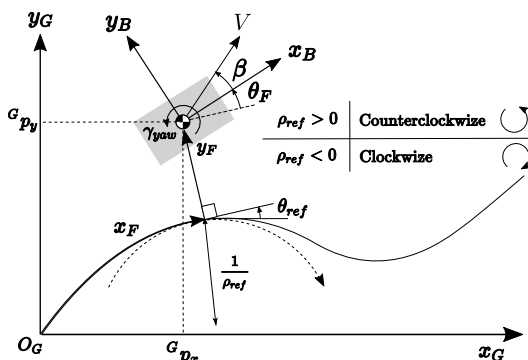


Fig. 2. Geometrical Relationship Between the Coordinates

TABLE I  
DEFINITION OF VARIABLES

Variable	Definition	Value [Unit]
$\beta$	Slip Angle of Vehicle Body	- [rad]
$\beta_f, \beta_r$	Slip Angles of Front, Rear Wheel	- [rad]
$\theta_F$	Yaw Angle between the Ref. Path	- [rad]
$\gamma_{yaw}$	Yaw Rate of Vehicle Body	- [rad/s]
$\delta$	Front Wheel Angle	- [rad]
$\rho_{ref}$	Curvature of Ref. Path	- [ $m^{-1}$ ]
$\theta_{ref}$	Yaw Angle of the Ref. in Global Frame	- [rad]
$B v_y$	Vehicle Longitudinal Velocity	- [m/s]
$V$	Vehicle Velocity	- [m/s]
$a$	Vehicle Acceleration	- [ $m/s^2$ ]
$l_f$	Distance from CG to the Front Axle	1.04 [m]
$l_r$	Distance from CG to the Rear Axle	1.56 [m]
$m$	Mass of Vehicle Body	1110 [kg]
$I_z$	Vehicle Moment of Inertia	1343 [ $kgm^2$ ]
$K_f$	Cornering Stiffness of Front Wheel	56023 [N/rad]
$K_r$	Cornering Stiffness of Rear Wheel	37942 [N/rad]

CG: center of gravity

## II. VEHICLE MODELS

### A. Definitions of variables and coordinates

First, the variables used to describe the models are defined in Table I. Before introducing the target vehicle models, the coordinate systems (Fig.2) used in vehicle models are defined. Note that this paper focuses only on the lateral control of the vehicle but not on the performance of speed nor acceleration control.

1) *Global coordinate*: The cartesian coordinate system in a fixed inertial frame to the map of driving scenes. The position vector in this coordinate is defined as  ${}^G P = [{}^G p_x, {}^G p_y]$ .

2) *Base coordinate*: The coordinate fixed on the moving frame at the position of the center of gravity (CG) of the car. The position vector in this coordinate is defined as  ${}^B P = [{}^B p_x, {}^B p_y]$ . The  $x_G$  axis direction is the same as the front of the vehicle.

3) *Frenet-Serret coordinate*: The coordinate fixed on the moving frame at the nearest point on the reference path from the car. The position vector is defined as  ${}^F P = [{}^F p_x, {}^F p_y]$ .  $x_F$  axis aligns with the tangent of the reference path and  ${}^F p_x$  means the trajectory length from the origin.  $y_F$  axis aligns with the reference path, and  ${}^F p_y$  value shows the lateral error between the car and the reference path.

See reference [17] for details of these coordinate systems.

### B. The Kinematic Ackermann Model

The first model tested in this paper is the Kinematic Ackermann Model (KAM). In conditions where the car turns along the stable circle at low speed, the Ackermann Geometry [8] (Fig. 3) exists in the global frame assuming no wheel slipping in the lateral direction. From geometrical relationship,

$$\rho = (l_f + l_r)/\delta, \quad (1a)$$

$$\gamma_{yaw} = V/\rho = \delta V/(l_f + l_r), \quad (1b)$$

$$\beta = l_r/\rho = \delta l_r/(l_f + l_r). \quad (1c)$$

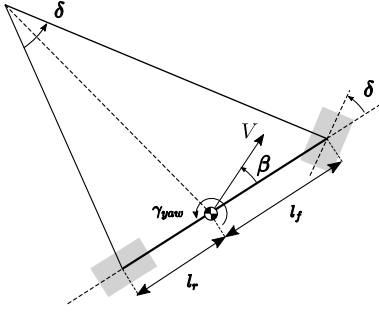


Fig. 3. Kinematic Ackermann Model

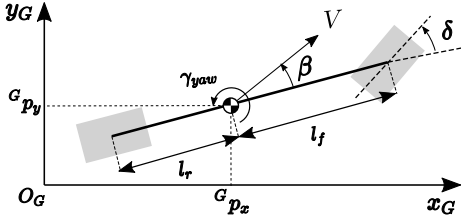


Fig. 4. Kinematic Bicycle Model

For path tracking, the KAM is transformed into Frenet-Serret frame as follows:

$$\begin{aligned} \frac{d}{dt} x_{\text{KAM}} &= \frac{d}{dt} \begin{bmatrix} {}^F p_y & \theta_F & {}^F p_x & V \end{bmatrix}^T \\ &= \begin{bmatrix} V\theta_F + \frac{l_r}{(l_f + l_r)} V\delta \\ -\rho_{ref} V + \frac{1}{(l_f + l_r)} V\delta \\ \frac{1}{V} \\ a \end{bmatrix}. \end{aligned} \quad (2)$$

See [8] for the details of the KAM. Note that the simple point mass model is used to express the simple longitudinal dynamics of the car in Eq.(2).

### C. The Kinematic Bicycle Model

The motion of the car at low speed can be described as the Kinematic Bicycle Model (Fig. 4) in an inertial frame. Driving speed in the global frame can be written as follows:

$$\dot{G}_{p_x} = V \cos(\theta_G + \beta), \quad \dot{G}_{p_y} = V \sin(\theta_G + \beta), \quad (3a)$$

$$\dot{\theta}_G = \frac{V}{l_r} \sin \beta, \quad \beta = \tan^{-1} \left( \frac{l_r}{l_f + l_r} \tan \delta \right). \quad (3b)$$

For path-tracking control purpose, Eq.(3) is described in Frenet-Serret frame as follows:

$$\begin{aligned} \frac{d}{dt} x_{\text{KBM}} &= \frac{d}{dt} \begin{bmatrix} {}^F p_y & \theta_F & {}^F p_x & V \end{bmatrix}^T \\ &= \begin{bmatrix} V \sin(\theta_F + \beta) \\ \frac{V}{l_r} \sin \beta - \frac{V \rho_{ref}}{D} \cos(\theta_F + \beta) \\ \frac{V}{D} \cos(\theta_F + \beta) \\ a \end{bmatrix}, \end{aligned} \quad (4)$$

where  $D = 1 - \rho_{ref} {}^F p_y$ .

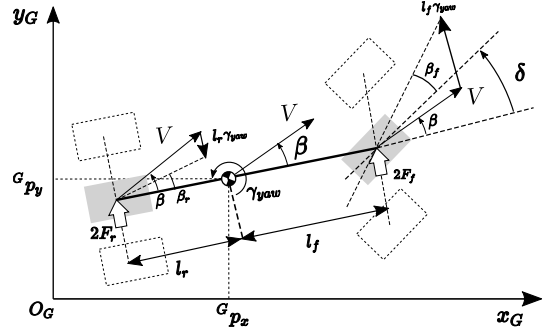


Fig. 5. Dynamic Bicycle Model

### D. The Dynamic Bicycle Model

The Dynamic Bicycle Model (DBM) is a well known lateral vehicle dynamics model in higher speed range which considers the effect of wheel slip angles. The equations of the DBM in the base coordinate can be written as follows:

$$\frac{d}{dt} \begin{bmatrix} {}^B v_y \\ \gamma_{yaw} \end{bmatrix} = \begin{bmatrix} -\frac{a_{11}}{V} & \frac{a_{12}}{V} - V \\ -\frac{a_{21}}{V} & \frac{a_{22}}{V} \end{bmatrix} \begin{bmatrix} {}^B v_y \\ \gamma_{yaw} \end{bmatrix} + \begin{bmatrix} b_1 \\ b_2 \end{bmatrix}. \quad (5)$$

For path tracking, the DBM can be described in Frenet-Serret coordinate as follows:

$$\begin{aligned} \frac{d}{dt} x_{\text{DBM}} &= \frac{d}{dt} \begin{bmatrix} {}^F p_y & \dot{{}^F p_y} & \theta_F & \dot{\theta}_F & {}^F p_x & V \end{bmatrix}^T \\ &= \begin{bmatrix} \dot{{}^F p_y} \\ -\frac{a_{11}}{V} \dot{{}^F p_y} + (a_{11} + a)\theta_F + \frac{a_{12}}{V} \dot{\theta}_F \\ \dot{\theta}_F \\ -\frac{a_{21}}{V} \dot{{}^F p_y} + a_{21}\theta_F + \frac{a_{22}}{V} \dot{\theta}_F \\ V \\ a \end{bmatrix} \\ &+ E^T \rho_{ref} + B^T \delta, \end{aligned} \quad (6)$$

where

$$a_{11} = \frac{2(K_f + K_r)}{m}, \quad a_{12} = -\frac{2(K_f l_f - K_r l_r)}{m}, \quad (7)$$

$$a_{21} = \frac{2(K_f l_f - K_r l_r)}{I_z}, \quad a_{22} = -\frac{2(K_f l_f^2 + K_r l_r^2)}{I_z}, \quad (8)$$

$$b_1 = \frac{2K_f}{m}, \quad b_2 = \frac{2K_f l_f}{I_z}, \quad (9)$$

$$E = [0, \rho_{ref}(a_{12} - V^2), 0, a_{22} - a, 0, 0]^T, \quad (10)$$

$$B = [0, b_1, 0, b_2 - a, 0, 0]^T. \quad (11)$$

### E. Improvement of the DBM in low driving speed range

The DBM has the drawback that it is not available at the driving speed  $V = 0$  because the model contains the term  $1/V$ , and the accuracy drops in the low speed range. Therefore, we approximate the  $1/V$  using soft normalization function [18] as Eq.12, and define the DBM improved in Low-speed range (DBM-L) as Eq.13 in order to improve its behavior at extremely low-speed range:

$$V_{inv} = \frac{1}{V + \alpha \ln(1 + \exp(-2\alpha V))}, \quad (12)$$

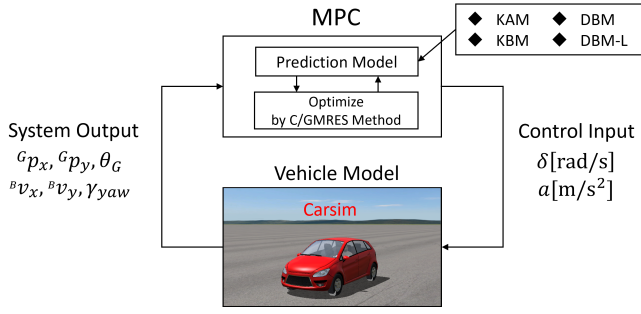


Fig. 6. Simulation architecture using MPC

where the constant  $\alpha = 1.0$  is used in this paper. Now the DBM-L can be described as follows:

$$\begin{aligned} \frac{d}{dt} x_{\text{DBM-L}} &= \frac{d}{dt} \begin{bmatrix} {}^F p_y & {}^F \dot{p}_y & \theta_F & \dot{\theta}_F & {}^F p_x & V \end{bmatrix}^T \\ &= \begin{bmatrix} {}^F \dot{p}_y \\ -a_{11} V_{inv} {}^F \dot{p}_y + (a_{11} + a) \theta_F + a_{12} V_{inv} \dot{\theta}_F \\ \dot{\theta}_F \\ -a_{21} V_{inv} {}^F \dot{p}_y + a_{21} \theta_F + a_{22} V_{inv} \dot{\theta}_F \\ V \\ a \end{bmatrix} \\ &+ E^T \rho_{ref} + B^T \delta. \end{aligned} \quad (13)$$

### III. COMPARISON OF CONTROL PERFORMANCE

#### A. Tested MPC controller

This paper clarifies the difference in the path-tracking performance of the MPC controller embedding different prediction models mentioned above. Figure 6 shows a simplified architecture of the model predictive path-tracking controller. The normal passenger car (B-class) in Carsim software (Mechanical Simulation Corp.) including a detailed vehicle dynamical model is used as the control target.

The optimization problem solved in each control interval is formulated as follows:

**Given:**

$$\hat{x}(0|t) = x(t), \quad x^{\text{ref}}, \quad S_f, \quad Q, \quad R, \quad (14)$$

**Find:**

$$\begin{aligned} \hat{x}(k|t), \quad k &\in \forall \{1, \dots, N\}, \\ \hat{u}(k|t) &= [\hat{\delta}(k|t), \hat{a}(k|t)]^T, \quad k \in \forall \{0, \dots, N-1\}, \end{aligned} \quad (15)$$

**Which minimize:**

$$J = \Phi(\hat{x}(N|t)) + \sum_{k=0}^{N-1} L(\hat{x}(k|t), \hat{u}(k|t)) \Delta t, \quad (16)$$

$$\Phi(\hat{x}(N|t)) = \frac{1}{2} (\hat{x}(N|t) - x_{\text{ref}})^T S_f (\hat{x}(N|t) - x_{\text{ref}}), \quad (17)$$

$$\begin{aligned} L(\hat{x}(k|t)) &= \frac{1}{2} (\hat{x}(k|t) - x_{\text{ref}})^T Q (\hat{x}(k|t) - x_{\text{ref}}) \\ &+ \hat{u}(k|t)^T R \hat{u}(k|t), \end{aligned} \quad (18)$$

**Subject to:**

$$\hat{x}(k+1|t) = \hat{x}(k|t) + \Delta t \frac{d}{dt} x_M \quad (19)$$

TABLE II  
PARAMETERS IN SIMULATIONS

	KAM, KBM	DBM, DBM-L
$\Delta t$	0.01s	0.01s
$N$	100	100
$S_f$	diag[ 10, 10, 0, 10 ]	diag[ 10, 1, 10, 1, 0, 10 ]
$Q$	diag[ 1, 1, 0, 1 ]	diag[ 1, 0.1, 1, 0.1, 0, 1 ]
$R$	diag[ 1, 1 ]	diag[ 0.1, 1 ]

TABLE III  
DRIVING SPEED AND CURVATURE FOR EVALUATION

Case	$v_{ref}$ [km/h]	R [m]
1	5	5
2	10	10
3	20	15
4	30	30
5	40	60
6	50	100
7	60	150
8	80	280
9	100	460
10	120	710

where  $x(t)$  is a state vector,  $S_f$ ,  $Q$ ,  $R$  are weight matrices. The dimension of  $x(t)$  and weight matrices differ depending on prediction models. The state equation  $\frac{d}{dt} x_M$  (Eq. 19) is also replaced depending on the target vehicle model for the evaluation.

#### B. Simulation and evaluation

The virtual car in CarSim drives along the reference paths shown in Fig.7 and 8 by using the MPC controller defined in the previous subsection. Applied prediction models are varied with the parameters shown in Table II for the evaluation.

Two of evaluation indices, mean value and maximum value of the lateral tracking error defined as:

$$E_{av} = \frac{\int_0^L |{}^F p_y| d{}^F p_x}{L}, \quad E_{max} = \max |{}^F p_y|, \quad (20)$$

are used for the evaluation of control performance.

#### C. Driving conditions

In this paper, 10 driving speed ranges listed in Table III (5[km/h] to 120[km/h]) are tested for each prediction model in order to cover the daily driving scene including low-speed urban driving and highway driving.

Two test track, (a). a half of oval track (Fig. 7), called oval-shaped path, and (b). a rectangular wave-like driving path (Fig. 8), called step-shaped path, are tested to evaluate the path-tracking performance. In (a), the curvature of the reference is changed depending on the driving speed as specified in Table III for the oval-shaped path. The applied curvature corresponding to a certain speed range is decided by referring to the standard of maximum curvature for road construction in Japan. In (b), the reference path is in a stepping manner to evaluate the step response performance of the path tracking.

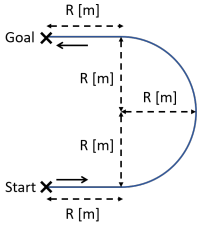


Fig. 7. Oval-Shaped Path

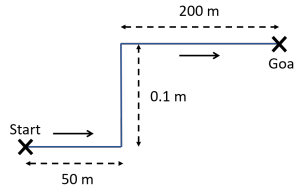


Fig. 8. Step-Shaped Path

#### D. Setting weight parameters

As the weight matrices in the evaluation function of MPC, the terminal cost  $S_f$ , the stage cost  $Q$ , and the penalty to the input  $R$ , are used in this study. In order to improve the tracking performance, the weight parameters on  ${}^F p_y$  and  $\theta_F$  were set to be large which are about 10 times the weight parameters on  ${}^F p_y$  and  $\theta_F$ , respectively, by trial and error. In addition, the terminal cost which the penalty of  $S_f$  is set to 10 times the value of  $Q$  for each state value in order to improve the stability of the controller in the receding horizon manner.

Note that the high accuracy path-tracking can not be achieved by just increasing the weight parameters on the lateral deviation  ${}^F p_y$ . Applying extreme penalties to certain state variable often leads to instability in the case of sudden reference change or the external disturbance as conventional state feedback control. In addition, this sometimes leads to numerical instability in C/GMRES computation.

### IV. EVALUATION RESULT

#### A. Availability of models in the various speed range

Figures 9 to 12 show the control performances of the MPC path tracking using different prediction models in various driving speeds. Note that all depicted points show the cases the car was able to follow the path, and the points are lacking if the car failed to track the path.

From the results shown below (Figs. 9 to 12), The KAM and the KBM can follow the reference only in 40 km/h and below on the oval-shaped path and 50 km/h and below on the step-shaped path. Note that these controllers were not able to follow the path even if the parameters in cost functions are fine-tuned. In contrast, the DBM and the DBM-L can follow both of the reference paths in all tested driving speed.

Since the DBM-L is equivalent to the DBM in the high-speed range, the DBM-L is available in a wide speed range as well as the conventional DBM. It is found that the DBM-L follows the tendency of the conventional DBM in the high-speed range from the results. Thanks to the soft normalization of the  $1/V$  term in the DBM-L, the model prevents the divergence of the computation in an extremely low-speed range successfully. As the result, the DBM-L enables the driving from 0km/h which is not possible with the conventional DBM. Figure 13 shows the time profiles of the states in a oval-shaped path tracking with 5km/h starting from a stop state ( $V = 0$  km/h).

As the summary of model comparison, Tab. IV classified the evaluation of each model regarding the availability and accuracy. From the results, the proposed DBM-L is the most applicable among the tested models in this study. Although the DBM-L shows the availability in all driving speed range, the tracking accuracy of the DBM and the DBM-L are degraded in the low-speed range compared to the KAM and the KBM. This result implies that the KAM and the KBM are suitable in the low-speed range if the MPC controller can be switched, and the DBM-L is a better option if the one MPC controller must cover the wide range of driving speed including stop-and-go. Another concern on the DBM and the DBM-L is that the accuracy in high-speed ranges are degraded compared to the medium speed range. In particular, as seen in Figure 10, both the DBM and the DBM-L have a relatively large tracking error of more than 1m when driving on the oval-shaped path at 120km/h. In this comparative study, the parameters in vehicle models nor the controller are not tuned depending on the driving speed for a fair comparison, however, the fine parameter tuning should be necessary to realize accurate path tracking in high-speed driving.

#### B. Computation time

The computation time of the optimization problem solved in each control frame are shown in Tab. IV. The computation time with the conventional DBM shows a larger value compared to the KAM and the KBM because the DBM has more state variables. On the other hand, the computational time with the DBM-L was smaller than that of the DBM. This is not natural because the DBM-L has the same dimension as the conventional one and includes a complex soft normalization function in it. We did not find the reason for this result at the moment, and it is necessary to dive into the detail of the numerical computation in C/GMRES method in order to investigate the reason in future work.

#### C. Control frequency setting

One of the benefits to introduce MPC controller is the prediction of the future state trajectory. If the control period and the number of prediction steps are increased, the input can be optimized by looking at longer future predictions. This emphasizes the advantage of MPC to cope with sudden changes in the path. On the other hand, it may also cause a decrease in tracking performance. Increasing the control period often causes instability of the behavior, especially in the DBM which handles the differential equations of the vehicle dynamics. The simple Euler approximation was used for the discretization of the DBM and the DBM-L in this paper and it is found that these models become unstable as the control period gets longer. Introduction of the bilinear transform or Lunge-Kutta algorithm may overcome these drawbacks by improving the prediction accuracy of the model.

In addition, the extension of the prediction horizon can also lead to numerical instability and too long prediction horizon is meaningless obviously because the prediction

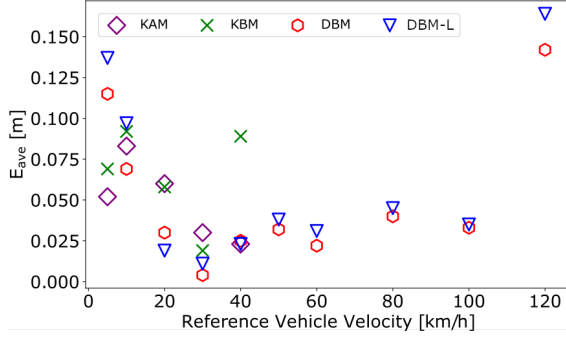


Fig. 9.  $E_{ave}$  of Oval-Shaped Path [m]

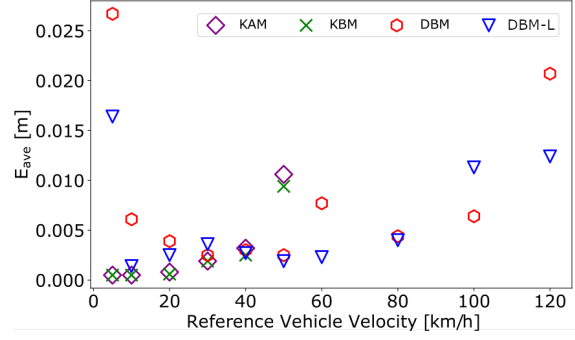


Fig. 11.  $E_{av}$  of Step-Shaped Path [m]

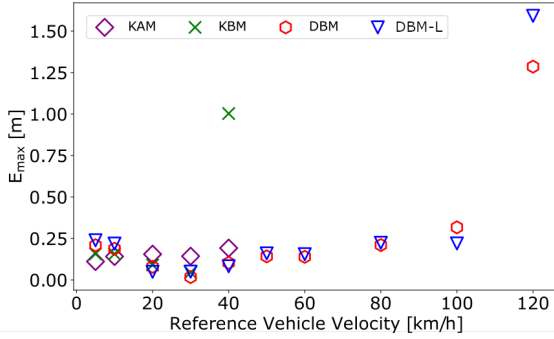


Fig. 10.  $E_{max}$  of Oval-Shaped Path [m]

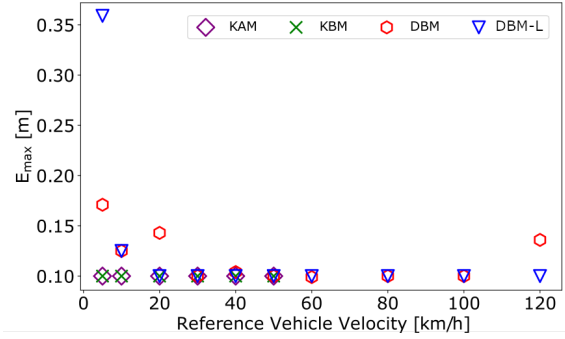


Fig. 12.  $E_{max}$  of Step-Shaped Path [m]

model can never perfectly predict the real vehicle behavior to be controlled. On the contrary, if the prediction interval is too short, the advantage of feed-forward control of MPC is lost and the behavior becomes similar to that of standard state feedback control.

The applied length of the prediction horizon and the control interval were determined by trial and error in this study, but it may be necessary to change the length depending on the type of the prediction model, the accuracy of the sensor, the route to be followed, and the speed range when the MPC is applied to a real vehicle.

1) *Parameter tuning:* Tuning of the weight parameters in the cost function of the optimization problem, which are  $R$ ,  $Q$  and  $S_f$ , is an important process in the controller design too. The parameters must be adjusted depending on the objective of the targeted driving task by taking a balance between the path-tracking accuracy and the riding comfort. From this viewpoint, it is desirable if the parameter setting can be determined independent of which model is applied to the prediction model. It is found that the fact that the MPC with either the KAM or the KBM could not follow in the high-speed range did not change even if different parameter sets were tried. Similarly, the DBM and the DBM-L were able to follow in various settings of these weight parameters. This implies that the stability itself does not improve by changing the cost function if the accuracy of the prediction model is poor, and it is natural considering the stability

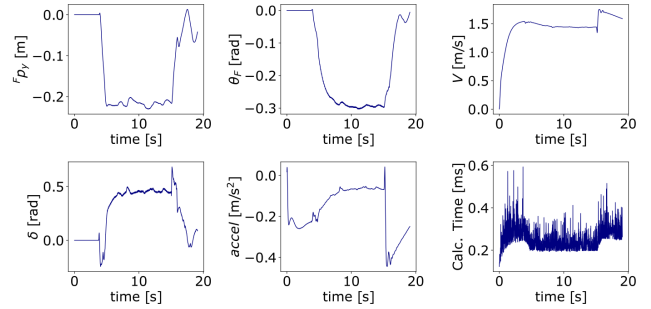


Fig. 13. Simulation Result using DBM-L and start from a  $V = 0$ km/h

analysis of the state feedback system. This also implies that the weight parameters can be adjusted more freely when the DBM and the DBM-L are used as the prediction model in the wide speed range in order to realize the desirable balance between the path tracking error and the smoothness of the behavior.

## V. CONCLUSIONS

This paper approached the automatic path-tracking control using a model predictive controller (MPC) and clarified the availability of the various prediction models in order to accelerate the development and the research of autonomous driving system. The conventional prediction models of lateral vehicle dynamics, the Kinematic Ackermann Model(KAM),

TABLE IV  
EVALUATION OF EACH VEHICLE MODEL

Evaluation Items		KAM	KBM	DBM	DBM-L
Tracking Accuracy	Low speed	A	A	C	B
	Mid. speed	C	C	A	A
	High speed	D	D	B	B
Ave. Calculation Time [ms]		0.219	1.011	1.684	0.573
Num. of Physical Parameters		2	2	5	5

The evaluations in the table are defined as follows:

A : High-accuracy tracking is possible in the speed range,

B : Tracking is possible in the speed range,

C : Tracking is possible only in a part of the speed range,

D : Tracking is impossible in the speed range.

the Kinematic Bicycle Model (KBM), and the Dynamic Bicycle Model (DBM), are tested in order to investigate the differences in the path tracking accuracy of the MPC controllers in various driving speed ranges. the DBM improved in Low-speed range (DBM-L) is proposed in order to overcome the drawbacks in the low-speed range of the conventional DBM and compared to other prediction models.

C/GMRES method was implemented in order to realize the real-time calculation of the nonlinear MPC including nonlinear prediction model.

As a result, it is found that the KAM and the KBM can be used only in a relatively low-speed range. The result is consistent with the conventional literatures which say that these models have less model accuracy in high-speed driving.

On the other hand, the DBM and the DBM-L can be used in a wide range from 5km/h up to 120km/h. In particular, the DBM-L proposed in this study enables the path tracking control including the stop-and-go situation thanks to the normalization in the extreme low-speed range, while also inheriting the advantages of the DBM in middle to high-speed ranges. This model can be considered as the most suitable prediction model to be used among the models tested in this study when the MPC must cover all the driving speed range.

On the other hand, the tracking performances of both the DBM and the DBM-L deteriorates in the high-speed range (especially at 120 km/h) compared to those of middle-speed range (20km/h to 100km/h). The improvement of the accuracy of the DBM-L and the total path tracking performance in the high-speed range is one of our future works.

Another future work is how to improve the path tracking performance in the low-speed range. There are two approaches for this problem, first one is to improve the DBM-L so that it can predict low-speed range, and another is to consider the smooth switching mechanism between the multiple vehicle models such as the DBM-L and the KAM.

## REFERENCES

- [1] M. Buehler, K. Iagnemma, and S. Singh, *The DARPA urban challenge: autonomous vehicles in city traffic*. Springer, 2009, vol. 56.
- [2] C. Samson, "Path following and time-varying feedback stabilization of a wheeled mobile robot," *Second International Conference on Automation, Robotics and Computer Vision*, vol. 3, 01 1992.
- [3] P. Hingwe and M. Tomizuka, "A variable look-ahead controller for lateral guidance of four wheeled vehicles," in *Proceedings of the 1998 American Control Conference. ACC (IEEE Cat. No.98CH36207)*, vol. 1, 1998.
- [4] D. Mayne, J. Rawlings, C. Rao, and P. Scokaert, "Constrained model predictive control: Stability and optimality," *Automatica*, vol. 36, no. 6, pp. 789 – 814, 2000.
- [5] R. L. Y. J. B. Z. Li, J. Deng and C.Y.Su, "Trajectory-tracking control of mobile robot systems incorporating neural-dynamic optimized model predictive approach," *IEEE Trans. on Sys., Man, and Cybernetics: Systems*, vol. 46, no. 6, pp. 740–749, 2015.
- [6] A. Koga, H. Okuda, Y. Tazaki, T. Suzuki, K. Haraguchi, and Z. Kang, "Realization of different driving characteristics for autonomous vehicle by using model predictive control," in *2016 IEEE Intelligent Vehicles Symp. (IV)*, 2016, pp. 722–728.
- [7] J. Ji, A. Khajepour, W. Melek, and Y. Huang, "Path planning and tracking for vehicle collision avoidance based on model predictive control with multiconstraints," *IEEE Trans. on Vehicular Tech.*, vol. 66, no. 2, pp. 952–964, 2017.
- [8] M. Abe, *Automotive Vehicle Dynamics*. Tokyo Denki University Press, 2008.
- [9] R. Rajamani, *Vehicle dynamics and control*. Springer Science & Business Media, 2011.
- [10] S. Oyeler, "The application of model predictive control (mpc) to fast systems such as autonomous ground vehicles (agv)," *IOSR Journal of Computer Engineering* 2278-0661, 2014.
- [11] X. Qian, A. de La Fortelle, and F. Moutarde, "A hierarchical model predictive control framework for on-road formation control of autonomous vehicles," in *2016 IEEE Intelligent Vehicles Symp. (IV)*, 2016, pp. 376–381.
- [12] C. J. Ostafew, A. P. Schoellig, T. D. Barfoot, and J. Collier, "Learning-based nonlinear model predictive control to improve vision-based mobile robot path tracking," *Journal of Field Robotics*, vol. 33, no. 1, pp. 133–152, 2016.
- [13] M. Werling and D. Liccardo, "Automatic collision avoidance using model-predictive online optimization," *Proceedings of the IEEE Conference on Decision and Control*, no. March, pp. 6309–6314, 2012.
- [14] F. Gritschneider, K. Graichen, and K. Dietmayer, "Fast trajectory planning for automated vehicles using gradient-based nonlinear model predictive control," *arXiv*, pp. 0–5, 2018.
- [15] P. Polack, F. Althé, B. d'Andréa Novel, and A. de La Fortelle, "The kinematic bicycle model: A consistent model for planning feasible trajectories for autonomous vehicles?" in *2017 IEEE Intelligent Vehicles Symp. (IV)*. IEEE, 2017, pp. 812–818.
- [16] T. Ohtsuka, "A continuation/gmres method for fast computation of nonlinear receding horizon control," *Automatica*, vol. 40, no. 4, pp. 563–574, 2004.
- [17] Y.-l. Liao, M.-j. Zhang, and L. Wan, "Serret-frenet frame based on path following control for underactuated unmanned surface vehicles with dynamic uncertainties," *Journal of Central South University*, vol. 22, pp. 214–223, 01 2015.
- [18] N. D. Ratliff, J. Issac, D. Kappler, S. Birchfield, and D. Fox, "Riemannian motion policies," 2018.